Nanoscale Reduction in Surface Friction of Polymer Surfaces Modified with Sc3 Hydrophobin from *Schizophyllum commune*

Rahul Misra,[†] Jun Li,[†] Gordon C. Cannon,[‡] and Sarah E. Morgan*[,†]

Department of Polymer Science, and Department of Chemistry and Biochemistry, The University of Southern Mississippi, Hattiesburg, Mississippi 39406

Received December 21, 2005; Revised Manuscript Received March 3, 2006

Hydrophobins are amphipathic self-assembling proteins secreted by filamentous fungi that exhibit remarkable ability to modify synthetic surfaces. Thin coatings of Sc3 hydrophobin isolated from the wood-rotting fungus *Schizophyllum commune* were prepared via spin coating and adsorption techniques onto polymeric surfaces. Surface morphology and nanotribological characteristics of the films were evaluated using lateral force microscopy (LFM) and nanoindentation techniques. This paper reports the first observation of reduction in nanoscale relative surface friction of Sc3 hydrophobin protein modified polymeric surfaces. Relative friction coefficients were dramatically reduced and hydrophilicity increased for polymer surfaces modified with Sc3 hydrophobin thin films. Morphology of the protein films as well as degree of surface modification was observed to be a function of film formation technique and composition of the substrate.

Introduction

Hydrophobins are small proteins (~100 amino acids) secreted by fungi that can self-assemble into a polymeric amphipathic membrane at interfaces and effect the reversal of the surface polarity. Hydrophobins play multiple roles in the development and reproduction of fungi, including fungal attachment to surfaces, stabilization and aid in emergence of fruiting bodies and aerial hyphae, and protective coatings for fungal structures.[1−3] Isolated hydrophobin proteins self-assemble from aqueous solution onto hydrophobic or hydrophilic surfaces and form a tightly bound membrane that is highly resistant to removal by solvents, denaturing agents, or changes in temperature or pressure. For example, a Teflon surface can be rendered hydrophilic by introduction into an aqueous solution of a class I hydrophobin (water contact angle decreases from 120° to ~30°),[4,5] and the resultant thin protein film is removed from the surface only by treatment with trifluoroacetic acid (TFA).[6,7]

The mechanism of hydrophobin self-assembly has been the subject of considerable research effort. The hydrophobin protein Sc3 from the wood-rotting fungus *Schizophyllum commune* has been the most widely studied hydrophobin and is the subject of the present study. It has been shown that isolated Sc3 dissolved in aqueous solution associates via two distinct mechanisms.[8] When air bubbles are introduced into hydrophobin solution, spontaneous self-assembly of hydrophobin occurs at the air−water interface, resulting in the formation of hydrophobin-stabilized dispersed microscopic air bubbles. These dispersions are highly stable, and the membranes can be disrupted only by treatment with TFA. In undisturbed hydrophobin solutions, on the other hand, less tightly associated aggregates form in a time-dependent manner. These loose aggregates can be converted to self-assembled membranes via vortexing. The assembled structures, however, do not disassemble over time to produce the loose aggregates. Thus, the method of preparation and handling of hydrophobin solutions is extremely important, and it is critical to employ freshly prepared solutions of known handling history for study of assembly and surface modification.

Hydrophobins are divided into two classes with different assembly behavior.[1,9,10] Class I proteins, such as Sc3, form assembled membranes that are extremely stable and can be disrupted only with TFA.[11] Class II hydrophobin assemblies, on the other hand, are responsive to a variety of stimuli, including denaturing agents, surfactants, and organic solvents.[12] The three-dimensional structure of a class II hydrophobin, HFBII from *Trichoderma reesei*, has recently been determined.[13,14] The authors propose that the molecular assembly process creates a "hydrophobic patch" on the outside of the assembly that is directed toward the hydrophobic surface and facilitates attachment to the surface. They suggest that a similar mechanism occurs for class I proteins. The extreme stability of class I assemblies in combination with their dramatic propensity to assemble, however, make them more difficult to analyze and characterize by conventional techniques. Recent studies of surface modification by HFBII and SC3 indicate that the class I Sc3 hydrophobin generally yields higher changes in surface character, as measured by water contact angle.[15]

Because of their remarkable assembly and surface modification behavior, hydrophobins have been suggested for a wide range of biomedical, technical, and personal care applications,[16−18] for example, to provide hydrophilic, improved biocompatibility, low-friction surfaces for biomedical devices. Due to the difficulties in isolating these proteins and their currently limited production, the greatest potential for initial application is in the area of high-value biomedical or personal care applications.[13] Recent studies indicate that hydrophobin has low cytotoxicity, and genetic engineering provides hydrophobin derivatives with improved biocompatibility.[19−21] Corvis et al.[22] demonstrated the utility of Sc3 hydrophobin for enzyme immobilization. Other potential high-value applications of hydrophobins were recently reviewed[23] and include use as antifouling or antibacterial coatings and emulsion stabilization aids for personal care products.

* To whom correspondence should be addressed. E-mail: sarah.morgan@usm.edu.

[†] Department of Polymer Science.

[‡] Department of Chemistry and Biochemistry.

10.1021/bm050983y CCC: $33.50 © 2006 American Chemical Society
Published on Web 04/07/2006

Low-friction surfaces are required in various biomedical applications including catheters, guide-wires, and other medical tools used in surgical procedures. Low friction not only helps to reduce chances of injury to tissues and membranes in contact with these devices, thereby facilitating smooth surgical procedures, but it also enhances long-term use of the devices. Conventionally, low-friction surfaces for biomedical devices are achieved either by using fluoropolymers for constructing these devices or by coating the surface with lubricants such as silicone oil, glycerin, or jelly-type materials. Although these lubricants render low friction to the surface initially, due to their weak adhesive properties they migrate to the surface and are unable to maintain their lubricious performance for longer duration. Once migrated to the surface these materials may be potential contaminants. Teflon fluoropolymer provides low friction; however, it exhibits poor biocompatibility, which is required for temporary or permanent implant devices.[20,21] This research work is an effort to address these problems by achieving stable, low friction, lubricious coatings with greater adhesion to the substrate using naturally derived hydrophobin. Although the biological function of hydrophobin proteins has been extensively studied and the morphology of the assembled films has been reported, the mechanical and tribological performance of these self-assembled thin films has not been studied. A thorough understanding of hydrophobin thin film tribomechanical performance is critical for their eventual use in biotechnology applications.

Atomic force microscopy (AFM) and nanoindentation techniques are increasingly employed for measurement and prediction of thin film properties, including friction, wear, surface roughness, adhesion, lubrication, hardness, and modulus.[24−27] Amonton's law describes friction at the macroscopic level, where the friction coefficient (μ) is the ratio of the frictional force (F_f) to the total normal force (F_n).[28,29]

$$\mu = F_f/F_n \tag{1}$$

In AFM measurements, polymeric materials deviate from this law due to effects from adhesion and surface tension.[27,30] The capillary forces between the tip and the liquid layer on the sample surface produce an adhesive force (F_a), which is added to the applied load (F_1) to give the total normal force applied to the sample.

$$\mu = F_f/(F_1 + F_a) \tag{2}$$

The apparent friction coefficient is obtained from the slope of a plot of F_f as a function of F_l.

Friction force measurements are obtained as a function of increasing applied load in contact mode using lateral force microscopy (LFM). In LFM, scanning is performed perpendicular to the long axis of the cantilever. Friction force is determined by evaluating the torque experienced by the cantilever in the forward and reverse scanning direction.[31−34]

In the present study, thin films of the hydrophobin Sc3 isolated from the wood-rotting fungus *S. commune* were prepared from aqueous solution using adsorption and spin-coating techniques. The two film preparation techniques represent an equilibrium process (adsorption) and a more energy-intensive process (spin coating) in which solvent is evaporated at a rapid rate to form an evenly distributed film.[35] Films were deposited onto two hydrophobic polymeric surfaces, polystyrene (PS) and a copolymer of benzoyl-1,4 phenylene and 1,3-phenylene (PBP), with the goal of achieving improved hydrophilicity and reduced friction. PS was chosen as the reference amorphous polymer material, as PS is a common amorphous thermoplastic used widely in biomedical and biotechnology applications, whose friction and hydrophobicity behavior at the macroscale are well understood. The nanotribological and nanomechanical performance of PS have recently been evaluated using nanoprobe techniques.[24,36] Newly commercialized PBP copolymers exhibit ultrahigh modulus and strength-to-weight ratios.[37] These high-performance polymers are under investigation for a wide range of applications, including biomedical applications such as magnetic resonance imaging (MRI)-transparent implants or dental composites. Recent studies of the macro and nanotribological properties of PBP in our laboratories demonstrated ultralow friction properties for this materials.[35] It is of further interest to explore the surface modification behavior of hydrophobin, specifically the friction reduction capabilities of hydrophobin thin films, as a function of substrate type and film preparation technique. The morphology, adhesion, and friction characteristics of hydrophobin thin films assembled onto these surfaces were evaluated via nanoprobe techniques.

Experimental Section

Materials. The hydrophobin protein Sc3 was isolated from the wood rotting fungus *S. commune* and purified according to previously published procedures.[38−40] Briefly, the fungus *S. commune* was grown as a 1 L standing culture in minimal medium.[41] Purification of the Sc3 hydrophobin that was secreted into the liquid media begins by separating the fungal material from the culture media by centrifugation. Crystalline ammonium sulfate and sodium phosphate are added to clear fungal culture supernatant. Purification of the hydrophobin is performed by hydrophobic interaction chromatography with ammonium sulfate solutions of progressively lower concentration buffered by sodium phosphate at pH 8.0. The collected fractions are dialyzed extensively against water. The obtained solution is then agitated thoroughly. The solution is then centrifuged resulting in small pellet of Sc3, and the supernatant is discarded. The pellet is dissolved in TFA and then dried under nitrogen and lyophilized for 12 h. After redissolving in phosphate buffer, the protein content is analyzed by the bicinchoninic acid assay[42] (Pierce Chemical) using bovine serum albumin as a standard according to the manufacturer's recommendations. Because Sc3 is prone to self-assemble in response to even the slightest agitation of the solution, prior to the experiment, Sc3 is treated with 100% TFA and then lyophilized, which is reported to disassemble any Sc3 complex.[11] The resultant lyophilized Sc3 was then dissolved in 20 mM sodium phosphate buffer (20 mM NaH_2PO_4, pH 7.0) to yield a final protein concentration of 30 μg/mL.

PS of weight average molecular weight of 280 000 g/mol was purchased from Aldrich. Polyphenylene copolymer (PBP), PARMAX 1200, was supplied by Mississippi Polymer Technologies, Bay St. Louis, MS. Mica disks (9.9 mm diameter, Ted Pella, Inc.) were used as the substrate for PS and PBP films.

Sample Preparation. Spin coating of PBP and PS solutions was performed using a KW-4A (CHEMAT Technology) spin coater onto freshly cleaved mica substrates. PBP was dissolved in benzyl chloride at 2 wt %, and PS was dissolved in tetrahydrofuran (THF) at a concentration of 20 mg/mL. A volume of 10 μL of polymer solution was deposited on the mica disk. Spin coating was performed in two successive stages, an initial stage at 500 rpm for 15 s followed by a second stage at 3000 rpm for 45 s. Samples were dried for 3 h in ambient air followed by drying in a vacuum oven for 12 h at 70 °C.

Hydrophobin film coatings were prepared onto spin-coated PS and PBP substrates via two methods: spin coating and adsorption. Spin coating was performed by depositing 10 μL of Sc3 hydrophobin aqueous solution (30 μg/mL) onto PS and PBP substrates and spinning at 750 rpm for 20 s. Samples were washed with deionized (DI) water and dried in air. The adsorption method involved complete coverage of the substrate polymer film surface with hydrophobin solution (30

CDV

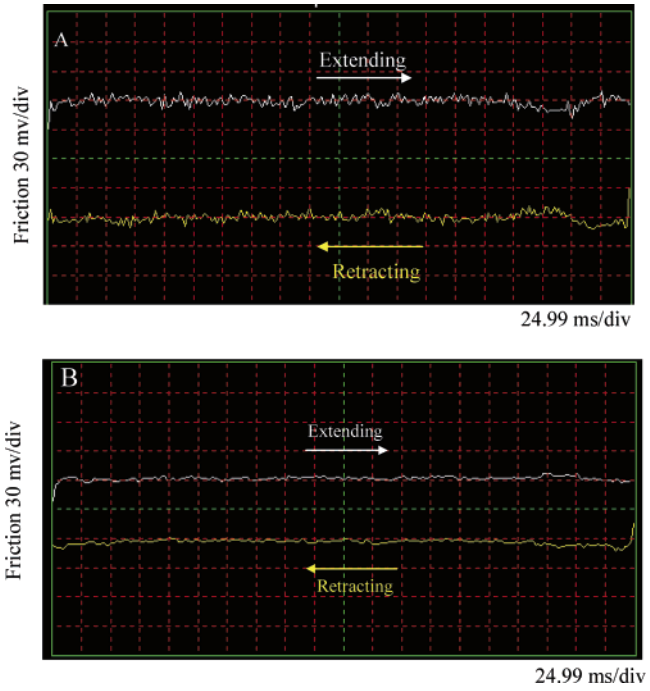

Figure 1. Friction loops for (A) neat PS and (B) Sc3 hydrophobin-coated PS.

μg/mL) for 12 h followed by (DI) water washing and drying in ambient air. Freshly prepared Sc3 solutions were employed for the studies in order to minimize time-dependent loose aggregate formation.[39]

Water Contact Angle Measurement. Surface advancing water contact angle measurements were conducted using sessile drop technique by a First Ten Angstroms (FTA, Portsmouth, VA) contact angle goniometer coupled with FTA 200 data analysis software.

AFM Surface Topography and Section Analysis. AFM evaluations were performed using a Dimension 3000 scanning probe microscope (Digital Instruments, Santa Barbara, CA). Probes for surface topography and friction measurements were purchased from Veeco probes, CA. Surface topography and roughness were obtained in tapping mode using an etched silicon probe, 125 μm long with a resonant frequency of 275 kHz, nominal force constant of 40 N/m, and a nominal tip radius of 10 nm. Height and phase images were collected simultaneously on 1 μm $\times$ 1 μm scan size with an image resolution of 256 $\times$ 256 pixels at a scan rate of 1 Hz. Surface roughness and section analysis was performed on 1 μm $\times$ 1 μm scan area for all the samples using Nanoscope version 5.30 r2 image analysis software.

Surface Friction Evaluation. Friction measurements were obtained by operating the AFM in the LFM mode using a triangular silicon nitride probe with a nominal spring constant of 0.58 N/m. Force−distance curves and friction signals were recorded at various setpoint voltages on a scan area of 5 μm $\times$ 5 μm and scan frequency of 1 Hz. The normal applied force was calculated from force−distance curves by the product of normal deflection of the cantilever and spring constant of the cantilever. Deflection of the cantilever is due to intermolecular forces between the tip and surface, which may be attractive and/or repulsive in nature.[30,31] In LFM, friction force is experienced in the direction opposite to the scan direction, while the normal force acts in the direction perpendicular to both the scan direction and the friction force direction. The cantilever experiences a torque imposed by the tip, which is recorded as a voltage signal. Voltage (mV) signal is then converted to friction force (nN) based on a calibration constant from a silicon wafer, which was determined to be 0.144 nN/mV using a reported friction coefficient of 0.06 for neat silicon wafer.[30] Trace and retrace images (Figure 1, parts A and B) are obtained in LFM while the tip moves over the stationary sample at a scan direction of 90°.

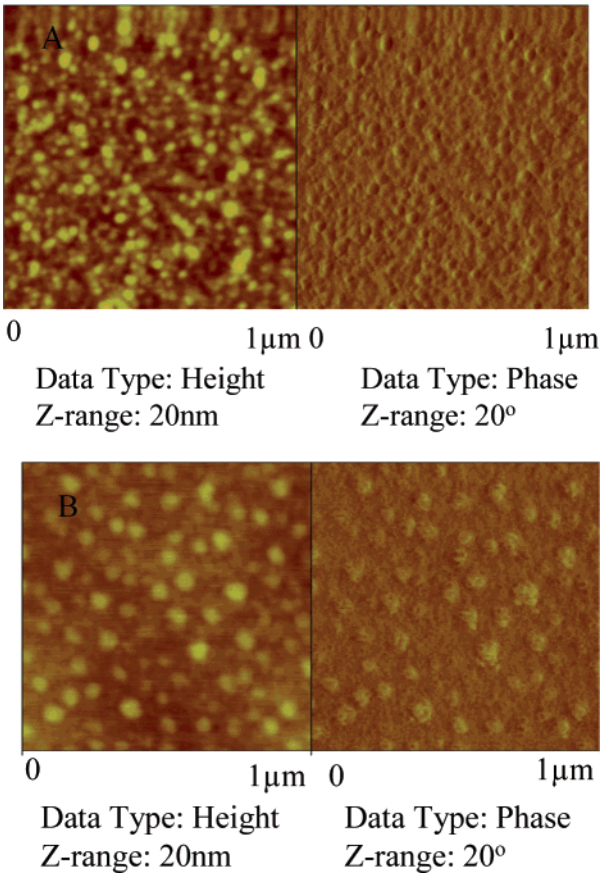

Figure 2. Height and phase image of Sc3 hydrophobin on PS: (A) adsorbed; (B) spin coated.

The frictional force for a given normal load is calculated as the mean value of the separation distance between the trace and retraces signals.[30−32]

Triboindenter Film Thickness Measurements. Nanoindentation thickness evaluations were performed on a Hysitron TriboIndenter with a three-sided diamond pyramid (Berkovich Type) tip using Triboscan 6.0 image analysis software. Tip calibration was performed using fused silica as the reference material. Normal force was applied to the surface at a loading and unloading rate of 10 μN/s with a 2 s hold period between the loading and unloading cycle. Nanoindentation was performed under closed loop with load control using the compliance method in which force−displacements curves are obtained during loading and unloading cycles. As the indenter presses into the surface the displacement is recorded as a function of the applied load.

Results and Discussion

Surface Morphology. Freshly cleaved mica and spin-coated PS and PBP films surfaces imaged by AFM are smooth and featureless, as expected.[35] A clear change in surface morphology is observed when Sc3 hydrophobin protein is deposited onto the spin-coated polymer films, with the appearance of spherical raised features (Figures 2 , parts A and B, and 3, parts A and B). The features appear in all films, whether prepared by adsorption or spin coating on PS or PBP, but their dimensions and distribution vary with film preparation technique, nature, and composition of the substrate. The density of these surface features appears to be greater for Sc3 films prepared by adsorption, presumably because the overnight adsorption technique allows adequate time for protein assembly to occur in an equilibrium-type process. Protein films prepared via spin coating exhibit features of more regular size and size distribution;

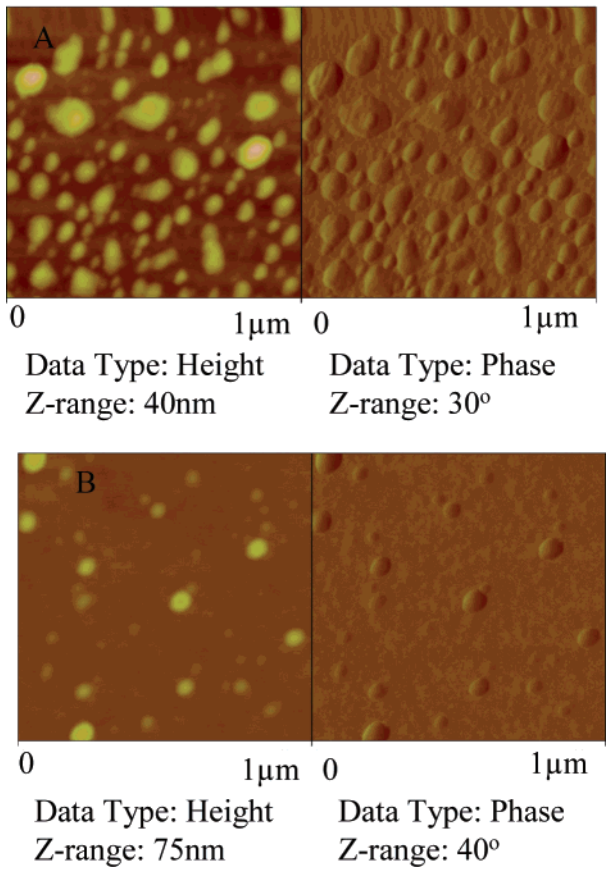

Figure 3. Height and phase image of Sc3 hydrophobin on PBP: (A) adsorbed; (B) spin coated.

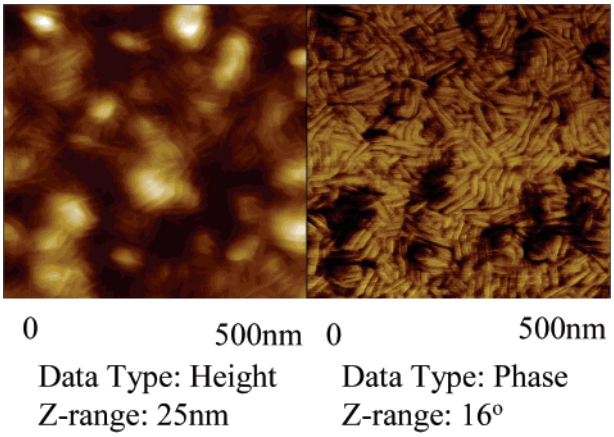

Figure 4. Height and phase image of the Sc3 hydrophobin rodlet pattern on a glass substrate.

however, they appear to exist as separate aggregates rather than as a continuous coating. Protein assembly may occur in solution during the spin-coating process prior to the deposition of the film on the surface, as hydrophobin assembly is readily induced by agitation of solution.[39] Similar morphological features are observed on PS and PBP substrates, but the features are larger and more widely dispersed on the PBP film. There is a clear contrast in morphology development on the hydrophobic polymer film surfaces in comparison to hydrophobin assembled onto a hydrophilic glass surface, as shown in the tapping mode image of Sc3 deposited onto a glass slide (Figure 4). On the hydrophilic glass surface, Sc3 hydrophobin self-assembles into rodlets approximately 5−12 nm wide by 20 nm in length, a typical pattern that has also been observed on fungal spore surfaces.[1,6,11,43]

Table 1. AFM Roughness Analysis for Neat and Sc3 Hydrophobin-Coated Polymer Substrates

sample	max height (nm)	mean roughness (nm)	rms roughness (nm)
freshly cleaved mica	1.35	0.11	0.15
PS on mica	2.61	0.21	0.26
Sc3 spin coated on PS	7.55	0.57	0.76
Sc3 adsorbed on PS	19.09	0.66	0.99
PBP on mica	10.01	0.23	0.30
Sc3 spin coated on PBP	17.21	0.49	0.91
Sc3 adsorbed on PBP	33.33	1.50	2.05

Surface roughness analysis for the samples is summarized in Table 1. Root mean square (rms) roughness for the neat PS and PBP films is approximately 0.3 nm, indicating a smooth surface that is only slightly rougher than the freshly cleaved mica surface (rms ~0.2 nm). The rms roughness is 3−6 times greater for polymer films modified with Sc3 hydrophobin, indicating the presence of the protein coating. Adsorbed Sc3 coatings produce rougher surfaces than spin-coated films, as would be predicted from the more irregular surface features observed in the tapping mode images of the adsorbed coatings. The greatest rms roughness value, 2.05 nm, was observed for Sc3 adsorbed onto the PBP surface, compared to an rms of 0.99 nm for Sc3 adsorbed onto the PS surface. The observed differences in the morphologies of the adsorbed protein films may be the result of differences in surface interactions and/or adhesion of the proteins to the polymer substrates, which in turn affect the protein self-assembly process and morphology of the resultant film.

Section analysis of the tapping mode images provides quantitative measurement of height and width of the observed features and provides further indication of differences in Sc3 protein interaction with different substrates. Multiple cross sections of the 1 μm × 1 μm tapping mode images were evaluated. Representative sections are shown in Figures 5, parts A and B, and 6, parts A and B. Hydrophobin protein films formed on PS surfaces yielded raised features of 2−3 nm in height, with diameters varying from 60 to 100 nm. Larger diameter features in greater density were observed for adsorbed coatings in comparison to those of spin-coated hydrophobin films. As the diameter of the globular Sc3 protein is estimated at approximately 3 nm,[20] these raised features would correspond to a single molecule thickness, with the large diameter arising from multiple molecule aggregates. Section analysis of Sc3 protein film on the PBP surface indicates raised features approximately 9 nm in height with diameters varying from 90 to 140 nm. These larger features correspond to multiple protein (or extended molecule) thickness, with a greater number of molecules involved to form the larger horizontal aggregates.

Nanoscale Friction Analysis. Measured friction force as a function of applied load yields linear plots for all samples (Figures 7 and 8). The relative coefficient of friction (COF) is obtained from the slopes of the lines and is summarized in Table 2. The hydrophobin-coated surfaces demonstrate very low friction, with reductions in COF of up to 80% in comparison to that of neat PS. Although the neat PBP substrate demonstrates a COF approximately half that of neat PS, all hydrophobin-coated surfaces yield similar relative COFs, with values ranging from 0.01 to 0.02, indicating similar coating effectiveness for all samples. Friction coefficients were measured repeatedly over

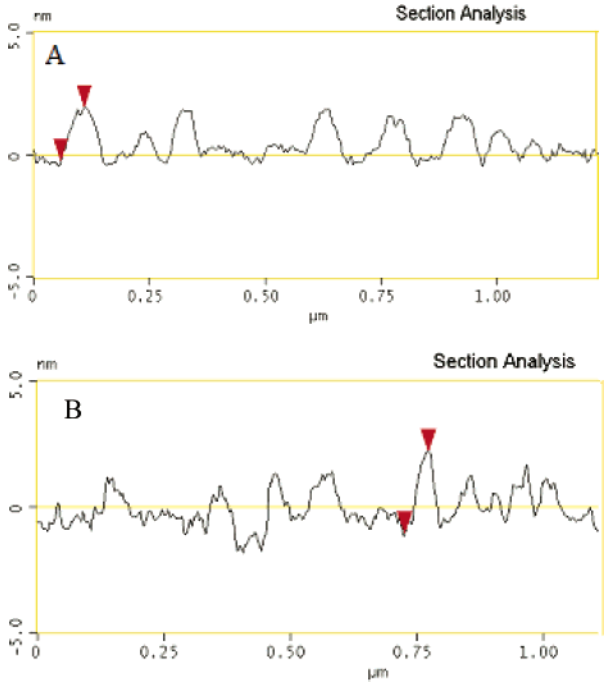

Figure 5. Section analysis of Sc3 hydrophobin on PS: (A) spin coated; (B) adsorbed.

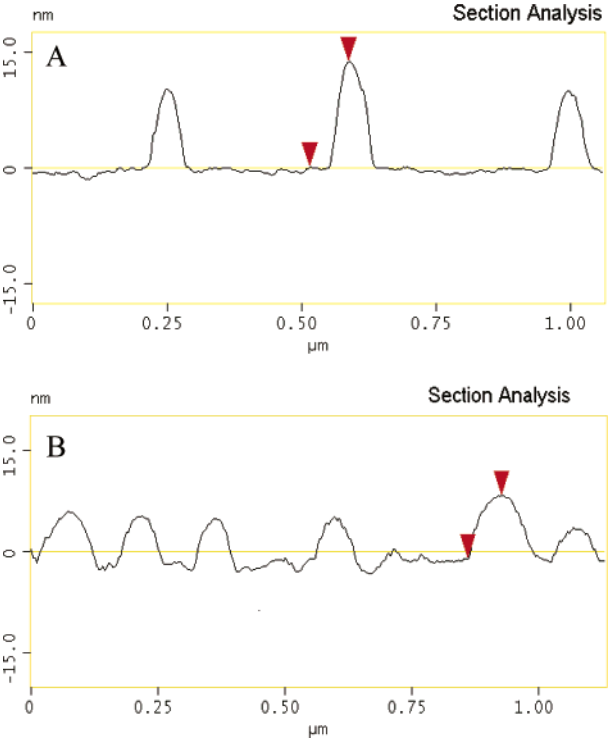

Figure 6. Section analysis of Sc3 hydrophobin on PBP: (A) spin coated; (B) adsorbed.

a period of several weeks with consistent results obtained in all measurements indicating stable attachment of Sc3 hydrophobin coating onto polymer surfaces.

Representative friction loops for the neat PS and Sc3 hydrophobin-coated PS films are shown in Figure 1, parts A and B. The gap between the trace and retrace friction curves is reduced for the hydrophobin-coated surface, indicating reduction in friction. The adhesive force (F_a) between the AFM tip and the substrate was estimated from force curves and from the intercept of the friction force versus applied load plots and is

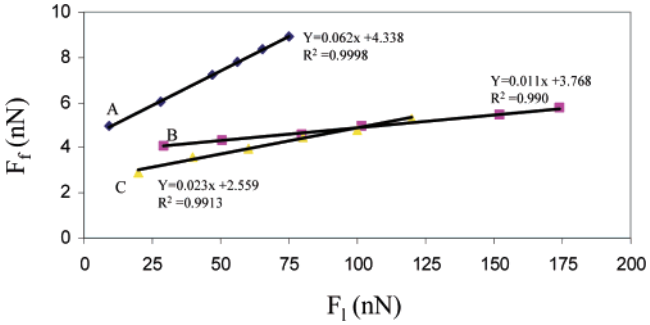

Figure 7. Friction force vs normal force plot for (A) neat PS, (B) Sc3 hydrophobin spin coated on PS, and (C) Sc3 hydrophobin adsorbed on PS.

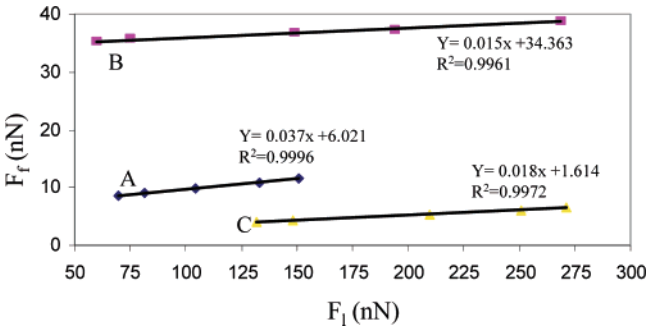

Figure 8. Friction force vs normal force plot for (A) neat PBP, (B) Sc3 hydrophobin spin coated on PBP, and (C) Sc3 hydrophobin adsorbed on PBP.

Table 2. Relative Value of COF and Adhesive Force for Neat and Sc3 Hydrophobin-Coated PS and PBP Films

sample	COF	adhesive force (nN) from force curve	adhesive force (nN) from friction plot
PS on mica	0.062	60.8	70.0
Sc3 spin coated on PS	0.011	326	342
Sc3 adsorbed on PS	0.023	96.1	111
PBP on mica	0.037	116	163
Sc3 spin coated on PBP	0.015	925	2290
Sc3 adsorbed on PBP	0.018	82.2	89.7

summarized in Table 2. Fairly good agreement is observed for adhesive force values obtained via the two methods. For PS samples, the adhesive force increases in the order neat PS < adsorbed coating Sc3 ≪ spin-coated Sc3, with the spin-coated sample showing dramatically higher adhesion. For PBP samples, the adhesive force increases in the order of adsorbed coating Sc3 < neat PBP ≪ spin-coated Sc3. Typical force curves for neat and Sc3-coated PBP substrates are shown in Figure 9, illustrating the dramatic increase in adhesive force for spin-coated hydrophobin surfaces. It would be expected that the greatest adhesive force would be exhibited for the most hydrophilic surface, due to interaction between the hydrophilic silicon nitride probe tip and the surface. However, the adhesive force trends do not match the trends obtained by macroscale water contact analysis (Table 3).

Water contact angle studies further illustrate the reversal of surface polarity provided by the assembled hydrophobin coating. Unmodified PS and PBP surfaces are hydrophobic, yielding contact angle values greater than 80°. Coating with Sc3 hydrophobin yielded dramatically reduced water contact angles. For the adsorbed protein coatings, the contact angle is 30−40°, as has been previously reported for Sc3 coatings on hydrophobic polymer substrates.[5] For the spin-coated protein coatings, the

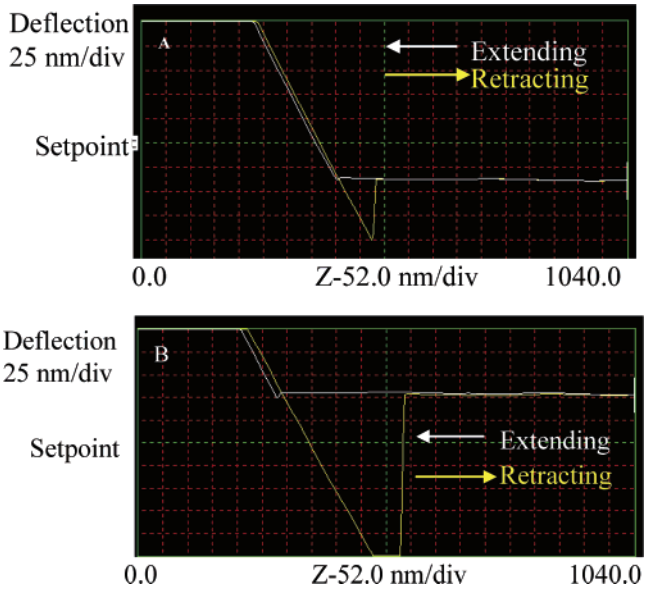

Figure 9. Force curves for (A) neat PS and (B) Sc3 hydrophobin-coated PS.

Table 3. Water Contact Angle Data for Unmodified and Sc3 Hydrophobin-Coated PS and PBP Film Surface

sample	contact angle (deg)
PS on mica	88
Sc3 spin coated on PS	62
Sc3 adsorbed on PS	28
PBP on mica	82
Sc3 spin coated on PBP	65
Sc3 adsorbed on PBP	40

contact angle is approximately 60°, indicating only partial coverage of the polymer surfaces or a difference in protein assembly during the spin-coating process.

The difference in observed trends for nanoprobe adhesive force measurements and water contact angle measurements could be due to several factors. First, the water contact angle measurement is a bulk measurement, where a surface area of several square millimeters is analyzed, while the nanoprobe force curve measurements analyze nanoscale areas. Second, differences in surface roughness may partially explain the differences. It has been shown that differences in surface roughness can affect water contact angle measured values[44−46] and may also be a factor in nanomechanical measurements.[47] Third, it has been reported that a second layer of hydrophobin may assemble on top of an assembled hydrophobin layer, causing a second reversal of the surface polarity[48] (i.e., hydrophobic ⟹ hydrophilic ⟹ hydrophobic). Thus, differences in surface roughness, related to differences in height of the raised features observed, may result from a distribution of multilayer assemblies, with different surface properties.

Film Thickness Analysis. The thickness measurements via triboindenter are summarized in Table 4. The thickness of the polymer spin-coated film substrates, which is indicated by the change in slope in the force−distance curve, is similar for both films, estimated as approximately 55 nm for neat PBP and 50 nm for neat PS. Representative force−distance curves for neat PBP, neat PS, and Sc3 spin coated onto the PBP and PS substrates are shown in Figures 10, parts A and B, and 11, parts A and B, respectively. Analysis of these curves indicates a protein layer thickness of approximately 12 nm on PBP, whereas

Table 4. Triboindenter Thickness Data for Unmodified and Sc3 Hydrophobin Spin-Coated PS and PBP Film Surface

sample	thickness (nm)
PS on mica	50
Sc3 spin coated on PS	20
PBP on mica	55
Sc3 spin coated on PBP	12

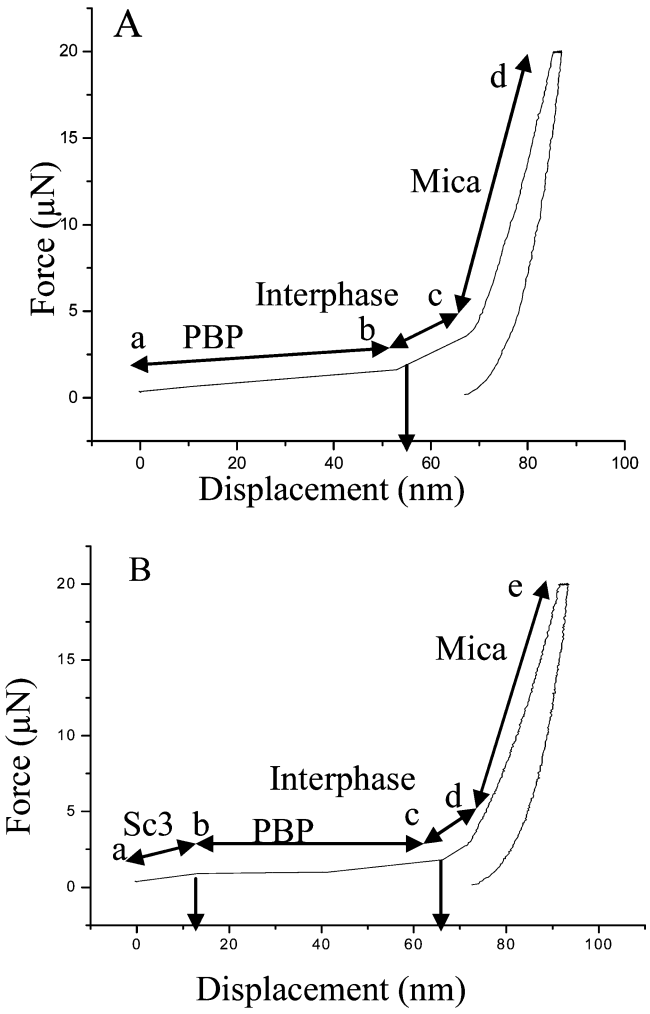

Figure 10. Triboindenter film thickness for (A) neat PBP and (B) Sc3 hydrophobin-coated PBP.

Sc3 coating on the PS substrate was estimated to be almost double this thickness, at 20 nm. Note that these measurements represent the thickness of the entire Sc3 film, while the section analysis measurements discussed in the Surface Morphology section represent only the height of the raised features on the surface of the film. Thus, Sc3 coatings on PBP have average thickness of 12 nm, with an rms roughness of 0.91 nm, while Sc3 coating on PS has average thickness of 20 nm, with an rms roughness of 0.76 nm. The differences in observed protein layer thickness, morphology, and roughness of the Sc3 coating on the two polymer substrates most likely explain the differences in measured water contact angle for the different coatings. Interestingly, however, the measured surface friction does not vary for the different coating types, with very low friction coefficients obtained for all Sc3-coated surfaces. This indicates that only a very thin Sc3 film is required for dramatic friction reduction on the polymer surface.

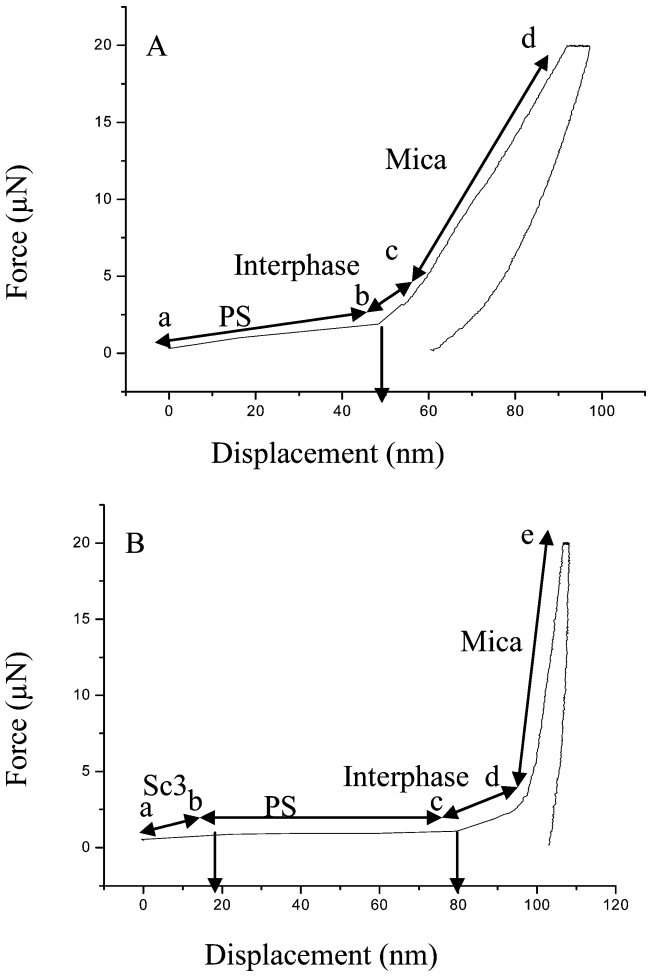

Figure 11. Triboindenter film thickness for (A) neat PS and (B) Sc3 hydrophobin-coated PS.

Conclusions

Thin and stable coatings of Sc3 hydrophobin, in the range of 10−20 nm, were prepared via spin coating and adsorption techniques from aqueous solution onto polymeric substrates. Polymeric surfaces with enhanced lubricity and reduced surface friction were obtained via Sc3 hydrophobin surface modification. Nanotribological analysis using LFM indicates ultralow relative friction coefficients for all hydrophobin-coated surfaces, in the range of 0.01−0.02 for measured relative friction coefficient. This represents a 70−80% reduction in friction coefficient in comparison to that of neat PS, and a 50−60% reduction in comparison to neat PBP, as the neat PBP has an initial friction coefficient that is substantially lower than that of PS. Friction measurements are reproducible, and the coatings provide stable friction reduction over a period of several weeks.

The hydrophilicity of the hydrophobin-coated polymer surfaces is significantly increased. Films prepared via the adsorption technique yielded more dense morphology, with more complete coverage of the polymer substrate, and greater hydrophilicity as measured via water contact angle. Nanoscale force of adhesion measurements, however, yielded different trends, with the spin-coated samples showing higher adhesion between the hydrophilic silicon nitride tip and the Sc3-coated surface. These differences may in part be explained by surface roughness effects and differences in the surface area measured in the different techniques. Morphology, thickness, and surface polarity of the Sc3 coatings can be altered by varying the substrate composition and coating conditions. The results indicate potential utility of hydrophobin coatings for personal care or biomedical applications requiring lubricious, low-friction surfaces, and further studies of these potential applications are underway.

Acknowledgment. This work was supported primarily by the MRSEC Program of the National Science Foundation under Award No. DMR 0213883. Additionally, acknowledgment is made to the donors of the American Chemical Society Petroleum Research Fund for partial support of this research and NSF MRI Award No. DMR-0421403. The authors thank Dr. Sergei Magonov (VEECO Industries, CA) for valuable discussions and inputs during this study.

References and Notes

(1) Wosten, H. A. B. *Annu. Rev. Microbiol.* **2001**, *55*, 625−46.
(2) Wessels, J. G. H. *Proc. Natl. Sci. Counc., Repub. China, Part B: Life Sci.* **1992**, *16* (3), 134−143.
(3) Wessels, J. G. H.; deVries, O. M. H.; Asgeirsdottir, S. A.; Schuren, F. H. J. *Plant Cell* **1991**, *3* (8), 793−799.
(4) Hong, C. K.; Benson, S. D.; Cannon, G. C.; McCormick, C. L.; Morgan, S. E. In *ANTEC Proceedings*, 2004.
(5) Wosten, H. A. B.; deVocht, M. L. *Biochim. Biophys. Acta* **2000**, *1469*, 79−86.
(6) Wosten, H. A. B.; Schuren, F. H. J.; Wessels, J. G. H. *EMBO J.* **1994**, *13* (24), 5848−5854.
(7) DeVocht, M. L. Ph.D. Dissertation, University of Groningen, 2001.
(8) Stroud, P. A.; Goodwin, J. S.; Butko, P.; Cannon, G. C.; McCormick, C. L. *Biomacromolecules* **2003**, *4* (4), 956−967.
(9) Wessels, J. G. H. *Annu. Rev. Phytopathol.* **1994**, *32*, 413−437.
(10) Wessels, J. G. H. *Adv. Microb. Physiol.* **1997**, *38*, 1−45.
(11) Wosten, H. A. B.; de Vries, O.; Wessels, J. G. H. *Plant Cell* **1993**, *5*, 1567−1574.
(12) Russo, P. S.; Blum, F. D.; Ipsen, J. D.; Yusuf, J. A.; Miller, W. G. *Can. J. Bot.* **1982**, *60*, 1414−1422.
(13) Linder, M. B.; Szilvay, G. R.; Setala, T. N.; Penttila, M. B. *FEMS Microbiol. Rev.* **2005**, *29*, 877−896.
(14) Hakanpää, J.; Paananen, A.; Askolin, S.; Nakari-Setälä, T.; Parkkinen, T.; Penttilä, M.; Linder, M. B.; Rouvinen, J. *J. Biol. Chem.* **2004**, *279*, 534−539.
(15) Lumsdon, S. O.; Grenn, J.; Stieglitz, B. *Colloids Surf., B* **2005**, *44*, 172−178.
(16) Scholtmeijer, K.; Wessels, J. G. H.; Wosten, H. A. B. *Appl. Microbiol. Biotechnol.* **2001**, *56*, 1−8.
(17) L'Oreal. French Patent FR2833490.
(18) Scholtmeijer, K.; Wessels, J. G. H.; Wosten, H. A. B. *Appl. Microbiol. Biotechnol.* **2001**, *56*, 1−8.
(19) Scholtmeijer, K.; Janssen, M. I.; Van Leeuwen, M. B. M; Van Kooten, T. G.; Hektor, H.; Wösten, H. A. B. *Bio−Med. Mater. Eng.* **2004**, *14*, 447−454.
(20) Scholtmeijer, K.; Janssen, M. I.; Gerssen, B.; De Vocht, M. L.; Van Leeuwen, M. B. M; Van Kooten, T. G.; Wösten, H. A. B.; Wessels, J. G. H. *Appl. Environ. Microbiol.* **2002**, *68*, 1367−1373.
(21) Janssen, M. I.; Van Leeuwen, M. B. M; Scholtmeijer, K.; Van Kooten, T. G.; Dijkhuizen, L.; Wösten, H. A. B. *Biomaterials* **2002**, *23*, 4848−4854.
(22) Corvis, Y.; Walcarius, A.; Rink, R.; Mrabet, N. T.; Rogalska, E. *Anal. Chem.* **2005**, *77*, 1622−1630.
(23) Hektor, H. J.; Scholtmeijer, K. *Curr. Opin. Biotechnol.* **2005**, *16*, 434−439.
(24) Bhushan, B. *Wear* **2001**, *251*, 1105−1123.
(25) Chen, Y. W.; Gan, D. J.; Kreiling, S.; Song, C. S.; Lu, S. Q.; Wang, Z. *J. Appl. Phys. A* **2003**, *76*, 129−132.
(26) Li, J.; Wang, C.; Shang, G.; Xu, Q.; Zhand, L.; Guan, J.; Bai, C. *Langmuir* **1999**, *15*, 7662−7669.
(27) Michel, D.; Kopp-Marsaudon, K.; Aime, J. *Tribol. Lett.* **1998**, *4*, 75−80.
(28) Howell, H. G.; Mazur, J. *J. Text. Inst.* **1953**, *44*, T59−69.
(29) Adamson, A. W. *Physical Chemistry*; Wiley: New York, 1990; pp 460−489.
(30) Bowden, F. P.; Taber, D. *Friction and Lubrication*; Oxford University Press: London, 1956.
(31) Ruan, J. A.; Bhushan, B. *J. Tribol.* **1994**, *116*, 378.
(32) Magonov, S. N. *Encyclopedia of Analytical Chemistry*; Meyers, R. A., Ed.; John Wiley & Sons: Chichester, U.K., 2000.
(33) Clark, H. A.; Plueddeman, E. P. *Mod. Plast.* **1963**, *40*, 133−135.
(34) Baselt, D. R.; Baldeshwielder, J. D. *J. Vac. Sci. Technol., B* **1992**, *10*, 2316−2322.

(35) Weill, A.; Dechenaux, E. *Polym. Eng. Sci.* **1988**, *28*, 945.
(36) Morgan, S. E.; Misra, R.; Jones, P. J. *Polymer*, in press.
(37) MPT Polymers. http://www.mptpolymers.com/ (accessed 10/01/05).
(38) Martin, G. G.; Cannon, G. C.; McCormick, C. L. *Biopolymers* **1999**, *49*, 621−633.
(39) Martin, G. G.; Cannon, G. C.; McCormick, C. L. *Biomacromolecules* **2000**, *1*, 49−60.
(40) Stroud, P. A.; Goodwin, J. S.; Butko, P.; Cannon, G. C.; McCormick, C. L. *Biomacromolecules* **2003**, *4* (4), 956−967.
(41) Dons, J. J. M.; de Vries, O. M. H.; Wessels, J. G. H. *Biochem. Biophys. Acta* **1979**, *563*, 100−112.
(42) Smith, P. K.; Krohn, R. I.; Hermanson, G. T.; Mallia, A. K.; Gartner, F. H.; Provenzano, M. D.; Fujimoto, E. K.; Goeke, N. M.; Olson, B. J.; Klenk, D. C. *Anal. Biochem.* **1985**, *150*, 76−85.
(43) DeVocht, M.; Scholtmeijer, K.; vander Vegte, E.; de Vries, O.; Sonveaux, N.; Wosten, H.; Ruysschaert, J.; Hadziioannou, G.; Wessels, J.; Robillard, G. *Biophys. J.* **1998**, *74*, 2059−2068.
(44) Lin, C. T.; Lin, K. L. *Appl. Surf. Sci.* **2003**, *214*, 243−258.
(45) Miller, J. D.; Veeramasuneni, S.; Drelich, J.; Valamamchill, M. R. *Polym. Eng. Sci.* **1996**, *36*, 1849−1955.
(46) Taniguchi, M.; Pieracci, J. P.; Belfort, G. *Langmuir* **2001**, *17*, 4312−4315.
(47) http://physicsweb.org/articles/world/18/2/9.
(48) Vander, V. W.; Vander, M. H. C.; Woosten, H. A.; Wessels, J. G.; Busscher, H. J. *Biophys. Chem.* **1996**, *57*, 253−260.

BM050983Y